Bioconjugate Chemistry

Communication

pubs.acs.org/bc

Conformational Modulation of in Vitro Activity of Cyclic RGD Peptides via Aziridine Aldehyde-Driven Macrocyclization Chemistry

Áron Roxin,[§,†] Juan Chen,[†] Conor C. G. Scully,[‡] Benjamin H. Rotstein,[‡] Andrei K. Yudin,*[,‡] and Gang Zheng*[,§,†]

[§]Department of Pharmaceutical Sciences and [‡]Department of Chemistry, University of Toronto, Toronto, Ontario, Canada

[†]Ontario Cancer Institute and Princess Margaret Hospital, University Health Network, Toronto, Ontario, Canada

Supporting Information

ABSTRACT: Here, we demonstrate a conjugation strategy whereby cyclic RGD-containing macrocycles are prepared using aziridine aldehydes, isocyanides, and linear peptides, followed by conjugation to a cysteamine linker. Our method involves site-selective aziridine ring-opening with the nucleophilic sulfhydryl group of cysteamine. Fluorescein was then efficiently conjugated to the primary amine of cysteamine by NHS-chemistry. This strategy may be expanded to provide easy access to a wide variety of fluorescent dyes or radiometal chelators. Modeling studies showed that aziridine aldehyde cyclization chemistry stabilized the RGD motif into the required bioactive conformation and that this cyclization chemistry modulated the geometry of macrocycles of different residue lengths. In vitro studies showed that cPRGDA and cPRGDAA both selectively bound to $\alpha_V\beta_3$-overexpressing U87 glioblastoma cells, and that cPRGDA had a better binding affinity compared to cPRGDAA. The improved binding affinity of cPRGDA was attributed to the fixed Pro-C$^{\alpha}$-Asp-C$^{\alpha}$ distance surrounding the stabilized RGD motif in cPRGDA.

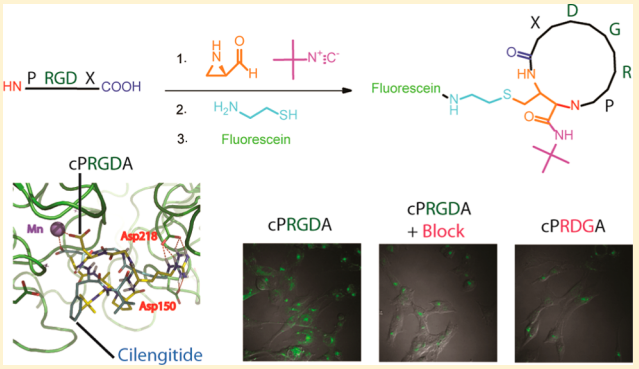

INTRODUCTION

Research into peptides targeting biomarkers associated with cancer actively pursues the creation of cyclic peptides that display specific biological activity and that can be functionalized for targeted imaging or therapy. A recent cyclization method developed in our laboratories employs amphoteric aziridine aldehydes and isocyanides to cyclize linear peptides through a rerouted Ugi reaction.[1] Aziridine aldehyde-driven cyclization proceeds rapidly, giving high yields at higher concentrations than is possible for conventional peptide cyclizations. This original procedure reported the conjugation of a thiolated coumarin fluorophore after cyclization and has since been refined to include several functional inputs. For instance, in addition to postcyclization fluorophore labeling, macrocycles have been labeled with a solvatochromic naphthalimide isocyanide during cyclization.[2] Most recently, novel thioester isocyanide reagents were developed with the goal of subsequent macrocycle−peptide ligation to access cycle-tail peptide scaffolds.[3] We sought to expand these recent conjugation strategies by developing a versatile modification chemistry whereby the conjugation of a wide variety of fluorophores, radiometal chelators, and other biological entities could be achieved.

Conventional amide-cyclized peptides often require additional lysine, cysteine, or glutamate residues to support side chain-selective conjugations. However, conjugations through these additional residues may hinder binding of the biologically relevant peptide regions[4−6] and often require cumbersome protection/deprotections protocols.[7−10] A method that enables one to constrain a linear epitope of interest into a macrocycle, while offering an exocyclic handle that can be modified at a late stage of synthesis without perturbing the desired conformation of the molecule,[11] is highly desirable. Here, we show a novel modification strategy wherein the thiol of cysteamine nucleophilically attacks aziridine aldehyde-cyclized macrocycles, resulting in aziridine ring-opening. Fluorescein was then conjugated to the macrocycles through the primary amine of cysteamine using *N*-hydroxysuccinimide (NHS)-chemistry (Scheme 1). This strategy removes the necessity of incorporating superfluous residues and allows the conjugation of a variety of biological entities containing carboxylic acid, isothiocyanate (ITC), or NHS functionalities by well-established amide coupling.

Arg-Gly-Asp (RGD)-containing peptides were chosen as a model for our investigations. The RGD motif is known to bind to the $\alpha_V\beta_3$ integrin receptor, which is overexpressed by several types of cancers and by tumor neovasculature.[12−15] To obtain biologically active RGD motifs, computer models of RGD-

Received: May 1, 2012
Revised: June 7, 2012
Published: June 18, 2012

Scheme 1. General Strategy for Synthesizing the Fluorescein-Labeled Aziridine Aldehyde-Cyclized RGD Macrocycles

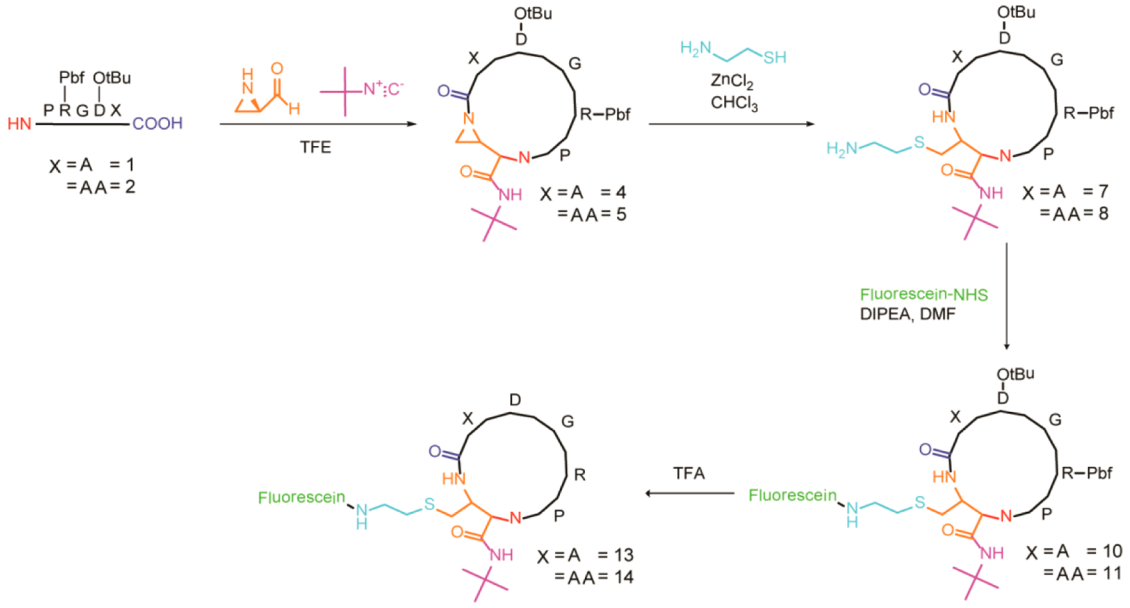

Chart 1. Novel Fluorescein-Labeled Macrocycles cPRGDA (13), cPRGDAA (14), and cPRDGA (15)

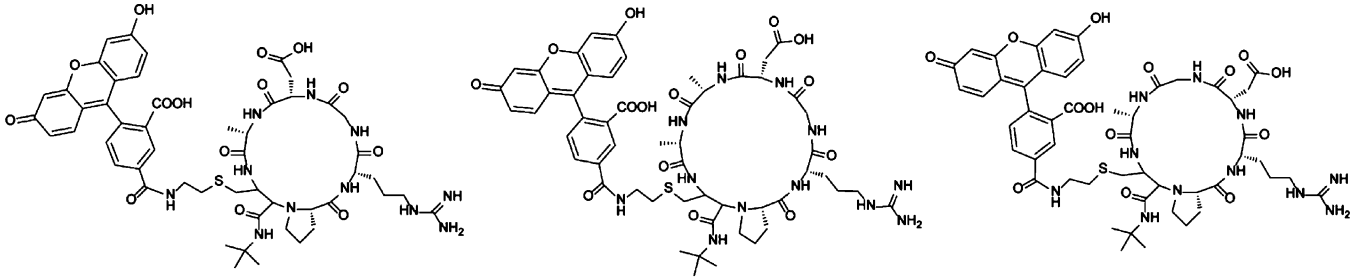

based aziridine aldehyde-cyclized pentapeptide and hexapeptide macrocycles were constructed in an attempt to recapitulate the observed backbone geometry from solution phase and crystallographic studies of potent integrin binding peptides. Docked conformations of promising RGD macrocycles and the $\alpha_V\beta_3$ integrin receptor were examined to investigate if these RGD macrocycles could attain binding geometries that were similar to the known high-affinity ligand cRGDf(N-Me)V (Cilengitide).[16−18] We proposed that if our RGD macrocycles could stabilize the RGD motif in a bioactive conformation similar to that of cRGDf(N-Me)V, then these peptides would be suitable for in vitro $\alpha_V\beta_3$ integrin-binding. Linear RGD-containing peptides were cyclized and labeled with fluorescein to experimentally validate the biological activity of the proposed functional macrocycles (Chart 1). Cell adhesion assays compared the binding affinity of the pentapeptide cPRGDA (**13**) and the hexapeptide cPRGDAA (**14**) to investigate how the geometry of these peptides correlated to their binding affinity for the $\alpha_V\beta_3$ integrin receptor of U87 glioblastoma cells. Confocal microscopy was then used to further investigate if these fluorescein-labeled macrocycles could specifically target the $\alpha_V\beta_3$ integrin receptor of U87 cells for in vitro cancer imaging. Our study provides a guide to experimentally verify the biological activity and specificity of our constrained RGD macrocycles proposed by computational geometry-based modeling that can be extended for screening other biologically active receptor-targeting motifs.

EXPERIMENTAL PROCEDURES

Chemicals. Organic solvents were purchased from Fisher Scientific and Sigma Aldrich. Amino acids and resins were purchased from Nova Biochem. Cysteamine, zinc chloride, L-serine, triphenyl phosphene (PPh_3), diisopropyl azodicarboxylate (DIAD), diisobutylaluminum hydride (DIBAL), *tert*-butyl isocyanide, and crystal violet were purchased from Sigma Aldrich. Fluorescein-NHS was purchased from Thermo Scientific. The chelator 1,4,7,10-tetraazacyclododecane-1,4,7-tris(*t*-butyl acetate)-10-acetate mono-succinimide ester (DOTA-NHS) was purchased from Macrocyclics. Pyropheophorbide-succinimide ester (Pyro-NHS) was synthesized following a previously published procedure.[19]

General Methods. Proton NMR was performed using a Bruker Ultrashield 400 Plus 400 MHz NMR. Mass spectrometry was performed using an Agilent Technologies 6130 Mass Spectrometer. The identity and purity of all peptide derivatives were assessed using a Waters 2695 HPLC with a Waters Delta Pak C18, 5 μm 3.9 × 150 mm column under reverse-phase conditions (0−100% acetonitrile in 0.1% TFA over 15 min at 0.8 mL/minute) while monitoring with a Waters 2996 photodiode array detector and a Waters Micromass ZQ mass spectrometer. Macrocycles were purified using a Waters Prep LC System with an Agilent 300SB-C3, 5 μm 9.4 × 250 mm column under reverse-phase conditions (0−100% acetonitrile in 0.1% TFA over 40 min at 3.0 mL/minute)

dx.doi.org/10.1021/bc300239a | *Bioconjugate Chem.* 2012, 23, 1387−1395

while monitoring with a Waters 2487 Dual λ absorbance detector set to 254, 300, 411, or 441 nm. Peptide derivatives were quantified spectrophotometrically by measuring the absorbance of Fmoc ((1:4) piperidine: DMF) or fluorescein (0.1 M NaOH) using a Varian 50 Bio UV−visible spectrophotometer. Binding affinity assays measured absorbance values using a Molecular Devices Spectra Max M5 plate reader. Confocal experiments were analyzed with an Olympus FV1000 laser confocal scanning microscope.

Synthesis of Unsubstituted Aziridine-Aldehyde (18). The unsubstituted aziridine-aldehyde (**18**) was synthesized as previously reported in our lab.[1,20] Briefly, 10 g (95 mmol) of L-serine was esterified to a serine propyl ester HCl salt (**16**) using 200 mL 1-propanol and 7.7 mL (106 mmol) $SOCl_2$. This reaction yielded 16.77 g (91.2 mmol) of precursor (96% yield). The identity was confirmed with ^{1}H NMR. ^{1}H NMR ($CDCl_3$, 400 MHz): δ 0.90 (t, J = 7.4 Hz, 3H), 1.62 (m, 2H), 3.51 (t, J = 4.1 Hz, 1H), 3.68 (dd, J = 10.9, 5.5 Hz, 1H), 3.76 (dd, J = 10.7, 4.0 Hz, 1H), 4.05 (t, J = 6.6 Hz, 2H).

The HCl salt (**16**) was converted to the free base (13.37 g or 90.9 mmol) using NH_4OH. A Mitsonobu reaction was performed using 23.85 g (90.9 mmol) of PPh_3 and 17.96 mL (90.9 mmol) of DIAD in anhydrous DCM at −10 °C for 3 h and at room temperature for 18 h. The workup required Et_2O precipitation to remove the white PPh_3O byproduct and a Kugelrohr apparatus (heated to 86 °C) to distill the aziridine propyl ester (**17**). This gave a 4.44 g (34.4 mmol) sample of this precursor (38% yield). The identity was confirmed with ^{1}H NMR. ^{1}H NMR ($CDCl_3$, 400 MHz): δ 0.92 (t, J = 7.4 Hz, 3H), 1.22 (m, 3H), 1.65 (m, 2H), 1.82 (d, J = 4.6 Hz, 1H), 1.96 (s, 1H), 2.49 (s, 1H), 4.08 (m, 2H).

The aziridine propyl ester (**17**) (2.0 g or 15.5 mmol) was reduced with 38.8 mL (38.8 mmol) of DIBAL (1.0 M in toluene) at −78 °C for 4.5 h. The reaction was quenched using MeOH after 2 h. Gelation was initiated with sat. $Na_2SO_{4\ (aq)}$ after 1 h and 45 min. The gel was filtered and washed with MeOH to give 532 mg (7.44 mmol) of the unsubstituted aziridine aldehyde dimer (**18**) (48% yield). Mass spectrometry was used to identify the product (ESI-MS: 143.1 (M+1) m/z). TLC was performed using acetonitrile/water (4:1) and showed an R_f = 0.4 (lit. R_f = 0.32).[1,20] $KMnO_4$ staining did not reveal any byproducts.

Manual Linear Peptide Synthesis. The linear peptides PRGDA (**1**), PRGDAA (**2**), PRDGA (**3**), PRGDK (**19**), and RGD (**20**) were synthesized on the solid-phase with 2-chlorotrityl chloride resin (loading ∼1.5 mmol/g) using standard Fmoc-chemistry. The amino acids Arg, Asp, and Lys had side chains protected by Pbf, OtBu, and Boc, respectively. Amide coupling of Fmoc-protected amino acids (3 equiv) was achieved after 2 h using HBTU (3 equiv) in (1:1) DCM/DMF containing 5% DIPEA (v/v). Resin capping was performed using 1-acetylimidazole (3 equiv) in a solution of (1:1) DCM/DMF containing 5% (v/v) DIPEA. Peptides were cleaved from the resin using (1:2:97) TFA/TIS/DCM after 2 h. Peptides were synthesized on a 250−550 μmol scale.

Aziridine-Driven Cyclization. The peptides PR(Pbf)GD(OtBu)A (**1**), PR(Pbf)GD(OtBu)AA (**2**), and PR(Pbf)D(OtBu)GA (**3**) were cleaved from the 2-chlorotrityl chloride resin as described and the N-terminal Fmoc was removed using standard piperidine cleavage. The peptides were precipitated from a minimal volume of DMF using cold Et_2O seven times. These peptides (10 μmol) were cyclized by the aziridine aldehyde-driven reaction[1,20] using 2.5 equiv of the unsubstituted aziridine-aldehyde dimer (**18**) and 3.5 equiv of *tert*-butyl isocyanide in TFE. The progress of cyclization reactions were assessed using HPLC-MS monitoring by integrating UV−vis spectra scanned at 254 nm. After 17−19 h, these cyclization reactions produced the desired macrocycles containing aziridine rings with the sequences PR(Pbf)GD(OtBu)A (**4**), PR(Pbf)GD(OtBu)AA (**5**), and PR(Pbf)D(OtBu)GA (**6**) where yields were estimated at ∼47%, ∼38%, and ∼43%, respectively. Mass spectrometry showed the production of **4** (ESI-MS: 960 (M+1) m/z), **5** (ESI-MS: 1031 (M+1) m/z), and **6** (ESI-MS: 960 (M+1) m/z). The reaction mixtures were precipitated using Et_2O. The crude mixtures were dried with a speed-vac and were stored at −20 °C.

Aziridine Ring-Opening with Cysteamine. The reaction crudes from the previous aziridine aldehyde-driven cyclization were dissolved in $CHCl_3$. Cysteamine was dissolved in DMSO to make a 3 mg/μL stock solution, while zinc chloride was dissolved in (95:5) $CHCl_3$/DMF to make a 0.1 mg/μL stock solution. Cysteamine and zinc chloride was added to the $CHCl_3$ solution containing the peptide crude. The molar ratio of peptide/cysteamine/zinc chloride was 1:3:1. The progress of this aziridine ring-opening reaction was assessed using HPLC-MS monitoring as described. Once the starting material was consumed, the reaction mixture was dried using a speed-vac. The crude was dissolved in a minimal volume of DMSO and was purified using a prep-HPLC. This gave the cysteamine-modified macrocycles with the sequences PR(Pbf)GD(OtBu)A (**7**), PR(Pbf)GD(OtBu)AA (**8**), and PR(Pbf)D(OtBu)GA (**9**) with yields of ∼23%, ∼33%, and ∼5%, respectively. The identity and purity of each product was confirmed using HPLC-MS (Figure S1, S2, and S3). Mass spectrometry showed the isolation of **7** (ESI-MS: 1037 (M+1) m/z), **8** (ESI-MS: 1108 (M+1) m/z), and **9** (ESI-MS: 1037 (M+1) m/z).

Amide Cyclization. The linear PR(Pbf)GD(OtBu)K(Boc) peptide (**19**) was cleaved from the 2-chlorotrityl chloride resin and the Fmoc-protecting group was removed as described. The NH-PR(Pbf)GD(OtBu)K(Boc)-COOH peptide (15 μmol) was cyclized using HBTU (1 equiv) and HOBt (1 equiv) while dissolved in 25 mL of DMF (1.76 mM) with 2.3% DIPEA (v/v). Reaction progress was monitored with HPLC-MS as described. The starting material was consumed within 20 h. The solution was aliquoted to 1.5 mL Eppendorf tubes and dried with a speed-vac. The dried product (**21**) was precipitated with DMF and Et_2O as described and dried with a speed-vac. The identity and purity of the product was confirmed using HPLC-MS (Figure S4). Mass spectrometry showed the product **21** (ESI-MS: 963 (M+1) m/z).

Fluorescein Conjugation. Fluorescein-NHS (1.5 equiv) was conjugated to the cysteamine-modified macrocycles in DMF containing 4% DIPEA (v/v) within 30 min. This reaction gave the side-chain protected fluorescein labeled macrocycles with the sequences PR(Pbf)GD(OtBu)A (**10**), PR(Pbf)GD(OtBu)AA (**11**), and PR(Pbf)D(OtBu)GA (**12**). ESI-MS(+) showed the production of **10** (ESI-MS: 1395 (M+1) m/z), **11** (ESI-MS: 1466 (M+1) m/z), and **12** (ESI-MS: 1395 (M+1) m/z). The Pbf and OtBu protecting groups were removed using TFA for 2 h. This side-chain deprotection step gave the final fluorescein-labeled macrocycles cPRGDA (**13**), cPRGDAA (**14**), and cPRDGA (**15**). These solutions were precipitated with Et_2O and purified using a prep-HPLC using the described method while detecting products with the 254 and 441 nm absorbance channels. HPLC-MS was used to determine the purity (>95% pure) and to confirm the identity

of each product (Figure S5, S6, and S7). Mass spectrometry showed the isolation of **13** (ESI-MS: 1087 (M+1) m/z), **14** (ESI-MS: 1158 (M+1) m/z), and **15** (ESI-MS: 1087 (M+1) m/z). The peptides were then quantified spectrophotometrically.

The Pbf, OtBu, and Boc protecting groups were removed from amide-cyclized PR(Pbf)GD(OtBu)K(Boc) peptide (**21**) using (95:5) TFA/DCM after 2 h. The production of the side-chain deprotected amide-cyclized PRGDK (**22**) was confirmed by mass spectrometry (ESI-MS: found 550 m/z). Fluorescein-NHS (1.3 equiv) was conjugated to the ε-NH_2 of Lys residue of the macrocycle (**22**) (7.5 μmol) in DMF containing 2.5% DIPEA (v/v) within 30 min. This solution was precipitated with Et_2O and purified using a prep-HPLC using the described method while detecting product with the 254 and 441 nm absorbance channels. HPLC-MS was used to determine the purity (>95% pure) and to confirm the identity of this fluorescein-labeled cyclic peptide amide-cPRGDK (**23**) (Figure S8). Mass spectrometry showed the isolation of amide-cPRGDK (**23**) (ESI-MS: 913 (M+1) m/z). The peptide was then quantified spectrophotometrically.

DOTA Conjugation. DOTA-NHS (3.3 equiv) was conjugated to the side-chain protected cysteamine-modified PR(Pbf)GD(OtBu)A macrocycle (**7**) (0.2 μmol or 1 equiv) in 50 μL of DMF containing 6% DIPEA (v/v) within 1 h. The crude was purified by prep-HPLC as described while detecting the product using a 254 nm absorbance channel. HPLC-MS was used to determine the purity (>90% pure) and to confirm the identity of the product (Figure S9). Mass spectrometry showed the production of cPRGDA-DOTA (**24**) (ESI-MS: 1423 (M^+) m/z).

Pyropheophorbide *a* Conjugation. Pyro-NHS (2 equiv)[19] was conjugated to the side chain-protected cysteamine-modified cPR(Pbf)GD(OtBu)A (**7**) (0.4 μmol or 1 equiv) in 70 μL of DMF containing 4% DIPEA (v/v) within 2 h. The crude was purified by prep-HPLC as described while detecting the product using 254 and 411 nm absorbance channels. HPLC-MS was used to determine the purity (>95% pure) and to confirm the identity of the product (Figure S10). Mass spectrometry showed the production of cPRGDA-Pyro (**25**) (ESI-MS: 1553 (M^+) m/z).

Computer Modeling. The cPRGDA (**13**) and cPRGDAA (**14**) peptides, as well as the amide-cPRGDK (**23**) peptide, were modeled using the Monte Carlo Multiple Minima (MCMM) algorithms implemented in *Macromodel*[21] using the OPLS2005 force field[22] and a Generalized-Born/Surface-Area (GB/SA) water model.[23] During this simulation, torsion angles of the macrocycles were varied randomly using a Monte Carlo procedure[24] and the conformational states were selected based on the Metropolis algorithm[25] according to the Boltzmann probabilities for each state based on its internal energy. We performed 1 000 000 steps of Monte Carlo sampling using 100 steps per each rotatable bond with retention of unique conformers. A 21 kJ/mol energy window was applied to discard high-energy conformers and we used a 0.5 Å maximum atom deviation cutoff to discard redundant conformers. An average structure was calculated for each peptide from their respective conformer families using *Macromodel*. Docking of cPRGDA, the N^{ε}-lysine-acetylated amide-cPRGDK and the highly studied cRGDf(N-Me)V peptide with the extracellular $\alpha_V\beta_3$ integrin protein (PDB entry 1L5G)[26] was performed using *Glide 5.7* (Schrodinger Inc.). The average ligand conformations used in the docking studies were obtained from the conformational search detailed above.

Binding Affinity. U87 glioblastoma cells were cultured in Corning 75 cm^2 flasks in MEM containing 10% FBS. Cells were allowed to reach ~70% confluence and were treated with trypsin containing EDTA for 15 min. The U87 cells (5×10^4 cells/well) were coincubated with various concentrations of the fluorescein-labeled cyclic peptides cPRGDA (**13**), cPRGDAA (**14**), cPRDGA (**15**), and amide-cPRGDK (**23**) (0−20 μM) on human vitronectin-coated 96-well plates (R&D Systems, Minneapolis, MN, USA) for 1 h at 37 °C. After washing, U87 cells were stained with 0.5% (v/v) crystal violet. The wells were washed and the absorbencies were measured at 627 nm in 0.1 M HCl using a plate reader.[27] IC_{50} values were calculated using Graph-Pad *PRISM* by a log(inhibitor) vs response three parameter nonlinear regression from $x-y$ scatter plots (bottom constraint at 18) of all normalized values from 3 independent experiments.

Confocal Microscopy. The U87 glioblastoma cells served as a positive cell line for the $\alpha_V\beta_3$ integrin receptor, while HT-29 colon cancer cells served as a negative cell line since these express low levels of the human $\alpha_V\beta_3$ integrin receptor.[28] U87 cells and HT-29 cells were cultured in Corning 75 cm^2 flasks in MEM and DMEM media, respectively, containing 10% FBS. Cells were allowed to reach ~70% confluence and were treated with trypsin containing EDTA for 15 min. Cells (3×10^4 cells/well) were transferred to 8-well Lab-Tek 155411 #1.0 borosilicate plates and were incubated with 10 μM solutions of fluorescein-labeled cPRGDA (**13**) and cPRGDAA (**14**) (0.5% v/v DMSO in media) for 2 h at 37 °C. The fluorescein-labeled cPRDGA scramble peptide (**15**) was used as a negative control, while the fluorescein-labeled amide-cPRGDK peptide (**23**) served as a positive control. The targeting specificity of cPRGDA and cPRGDAA was investigated by blocking the $\alpha_V\beta_3$ integrin receptor of U87 cells with a 50-fold molar excess of the linear RGD peptide (**20**). Laser confocal scanning microscopy was then performed with excitation wavelength of 488 nm using 5% laser power, PMT voltage of 760 V, and 120 μM pinhole diameter.

RESULTS

Aziridine Ring-Opening and Fluorophore/Chelator Conjugation. The general synthetic strategy included four distinct steps: (1) aziridine aldehyde-driven cyclization of linear peptides, (2) aziridine ring-opening by a heterobifunctional linker, (3) dye conjugation, and (4) full deprotection of amino acid side chains. The linear peptides with the sequences PR(Pbf)GD(OtBu)A, PR(Pbf)GD(OtBu)AA, and PR(Pbf)D-(OtBu)GA were successfully cyclized by our recently reported aziridine aldehyde-driven cyclization chemistry. Cysteamine was attached to these macrocycles by zinc chloride-catalyzed aziridine ring-opening. The cysteamine-modified macrocycles (**7**, **8**, and **9**) were then conjugated to fluorescein-NHS using DIPEA in DMF in 30 min (**10**, **11**, and **12**). The side-chain protecting groups were then removed using TFA to produce cPRGDA (**13**), cPRGDAA (**14**), and cPRDGA (**15**). We also extended the exocylic conjugation of the cysteamine-modified macrocycles to other reporters. The radiometal chelator DOTA was efficiently conjugated to the free amine of cysteamine on the macrocycle PR(Pbf)GD(OtBu)A (**7**) using NHS-chemistry (**24**). The multimodal fluorescent dye, photosensitizer, and radiometal chelator pyropheophorbide *a* was similarly con-

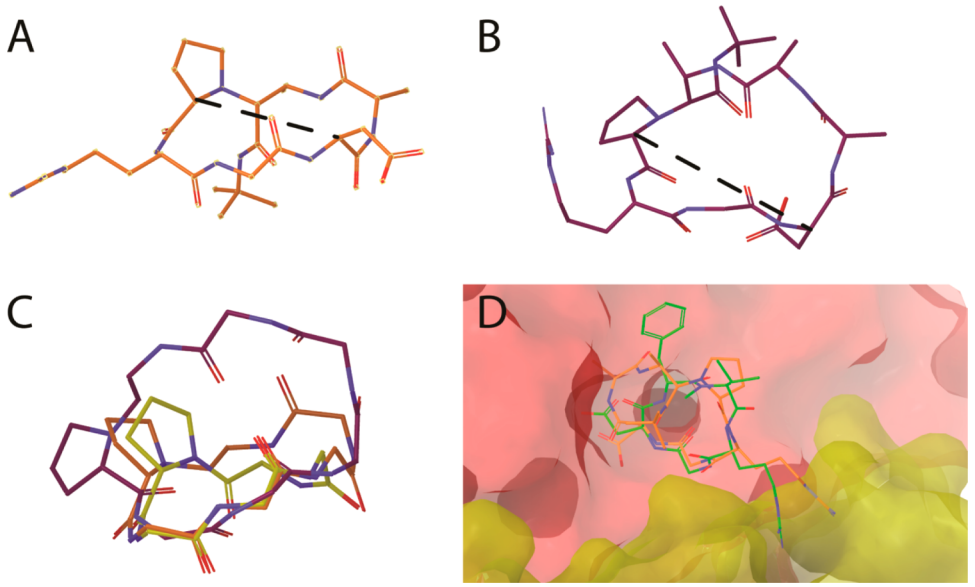

Figure 1. 3D models of (A) cPRGDA (orange) and (B) cPRGDAA (purple) separately showing Pro-C^{α}–Asp-C^{α} vectors and (C) overlaid with amide-cPRGDK (yellow). The cPRGDA peptide (orange) was overlaid with cRGDf(N-Me)V (green) in a docked configuration with the $\alpha_V\beta_3$ protein to illustrate structural similarity at the RGD-motif.

jugated to the free amine of cysteamine on the macrocycle PR(Pbf)GD(OtBu)A (**7**) using NHS-chemistry (**25**).

Computer Modeling. *Macromodel* was used to generate conformational ensembles of cPRGDA (**13**), cPRGDAA (**14**), and amide-cPRGDK (**23**). The average conformations of cPRGDA (Figure 1A), cPRGDAA (Figure 1B), and the amide-cPRGDK were analyzed to investigate suitability for binding to the $\alpha_V\beta_3$ integrin receptor. A preliminary study indicated that the pentapeptides, cPRGDA and amide-cPRGDK, preferred a backbone conformation that overlaid well with the RGD motif of cRGDf(N-Me)V (bound to the extracellular $\alpha_V\beta_3$ integrin protein (PDB: 1L5G)[26]) (Figure 1D), while the hexapeptide cPRGDAA showed significant backbone deviation in this area (Figure 1C). Conformational searches generated between 233 and 368 conformers for each of these macrocycles from which the mean Pro-C^{α}–Asp-C^{α} distances within cyclic peptides cPRGDA, cPRGDAA, and amide-cPRGDK (Table 1) were

Table 1. Calculated Pro-C^{α}–Asp-C^{α} Distances of Macrocycles Using Averaged Conformer Geometries

peptide	Pro-C^{α}–Asp-C^{α} distance (Å)	N^a
amide-cPRGDK	5.24 ± 0.15	368
cPRGDA	6.11 ± 0.17	264
cPRGDAA	8.37 ± 0.24	233

[a]Number of generated conformers.

calculated. Both cPRGDA and cPRGDAA contain a γ-turn-like backbone conformation similar to cRGDf(N-Me)V at the RGD motif (Arg-C^{α}–Asp-C^{α} < 7 Å). However, the cycle topology is significantly different when the residue preceding the RGD motif is included in the backbone comparison. The Val-C^{α}-Asp-C^{α} distance was measured at 6.9 Å in the crystal structure of cRGDf(N-Me)V which is similar to the distance calculated for Pro-C^{α}–Asp-C^{α} in cPRGDA (6.1 Å). The Pro-C^{α}–Asp-C^{α} distance in cPRGDK is shorter (5.2 Å) and is much longer in cPRGDAA (8.7 Å). This suggests that differing peptide backbone topology could account for the enhanced binding of the RGD-motif of cPRGDA to the $\alpha_V\beta_3$ integrin binding site compared to the larger cPRGDAA.

Ligand docking to the extracellular $\alpha_V\beta_3$ integrin protein showed that cPRGDA and the N^{ε}-acetyl-lysine analogue of amide-cPRGDK possessed similar stabilizing binding interactions to cRGDf(N-Me)V from the crystal structure. The Lys residue of amide-cPRGDK (**22**) was N^{ε}-acetylated in its docking study to mimic the presence of fluorescein in amide-cPRGDK (**23**). It was found that cPRGDA and cRGDf(N-Me)V docked to the $\alpha_V\beta_3$ integrin protein through their respective Arg residues to Asp150 and Asp218 of $\alpha_V\beta_3$ and through their Asp residues to Mn1 (Figure 2A). The N^{ε}-acetyl-

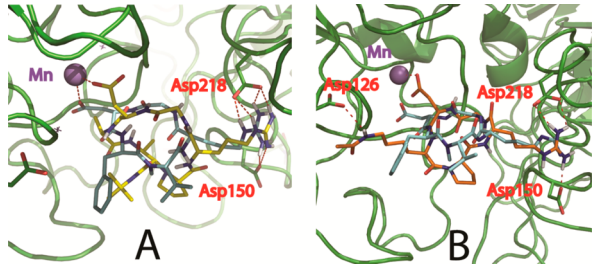

Figure 2. 3D modeling showing the comparative docking interactions of (A) cPRGDA (yellow) and cRGDf(N-Me)V (blue) and (B) amide-cPRGDK (orange) and cRGDf(N-Me)V (blue) with the extracellular binding regions of the $\alpha_V\beta_3$ integrin receptor.

lysine of the amide-cPRGDK analogue formed contacts to the same residues and also to Asp126 through the amide proton of the N^{ε}-acetyl-lysine residue (Figure 2B). Heavy atom distances between the respective docking regions of the $\alpha_V\beta_3$ integrin protein to cPRGDA, amide-cPRGDK, and cRGDf(N-Me)V were calculated (Table 2). These measurements showed that, while cPRGDA and cRGDf(N-Me)V used all three nitrogen atoms of their respective Arg residues for optimal binding to Asp150 and Asp218, the binding mode of the Arg of amide-cPRGDK is inferior. This observed binding mode uses two of

dx.doi.org/10.1021/bc300239a | *Bioconjugate Chem.* 2012, 23, 1387–1395

Table 2. Calculated Heavy Atom Distances between Macrocycles and the Extracellular Binding Regions of the $\alpha_V\beta_3$ Integrin Receptor

peptide	ligand atom	receptor atom	heavy atom distance (Å)
cPRGDA	Asp-OD	Mn1	2.1
	Arg-NE	D218-OD1	3.1
	Arg-NZ1	D218-OD2	3.1
	Arg-NZ2	D150-OD	3.2
amide-cPRGDK	Asp-OD	Mn1	2.1
	Arg-NZ1	D218-OD1	3.1
	Arg-NZ1	D218-OD2	2.9
	Arg-NZ2	D150-OD	3.0
	Ac-Lys-NZ	D126-OD	3.6
cRGDf(N-Me)V	Asp-OD	Mn1	2.7
	Arg-NE	D218-OD1	2.9
	Arg-NZ1	D218-OD2	2.8
	Arg-NZ2	D150-OD	3.3

its three available nitrogen atoms to bind to the dual aspartate motif of the integrin.

Binding Affinity. With computational insights in hand, the binding affinity of each fluorescein-labeled RGD-macrocycle for the $\alpha_V\beta_3$ integrin receptor was investigated experimentally using competitive cell adhesion assays. The peptide concentration-dependent displacement of U87 cell adherence from vitronectin-coated wells was used to calculate the respective IC_{50} values for fluorescein-labeled macrocycles cPRGDA (**13**), cPRGDAA (**14**), and amide-cPRGDK (**23**). The IC_{50} value of these RGD-containing macrocycles was on the same order (low μM) as previously reported amide-cyclized RGD sequences analyzed by this competitive cell adhesion method (Table 3).[27]

Table 3. Cell Adhesion Competition Assay Summary of IC_{50} Values of Fluorescein-Labeled Macrocycles

peptide	log IC_{50}[a] (M)	SE[b] (log M)	IC_{50}[c] (μM)
amide-cPRGDK	−5.114	±0.2	7.7
cPRGDA	−5.381	±0.2	4.2*
cPRGDAA	−4.955	±0.06	11.11*
cPRDGA	n.d.[d]	n.d.[d]	-

[a]Calculated in Graph-Pad *PRISM* using a log(inhibitor) vs response, three parameter nonlinear regression from an $x-y$ scatter plot (bottom constraint at 18) of all normalized values from 3 independent experiments. [b]Standard error calculated for log IC_{50} presented as log of molar concentrations. [c]Transformed from log IC_{50}. [d]n.d., Not determined. *Significantly different using a two-tailed unpaired t test ($p < 0.05$).

Though cRGDf(N-Me)V was not tested in this study, a review by Rüegg et al. reported that Cilengitide displays a similar $\alpha_V\beta_3$ integrin binding affinity (IC_{50} ~1 μM) to displace $\alpha_V\beta_3$ integrin-expressing cells from adhering to vitronectin.[29] The IC_{50} of cPRGDA (4.2 μM) was significantly lower compared to cPRGDAA (11.1 μM, $p < 0.05$) (Table 3). These differential IC_{50} values were attributed to modulated geometries as a result of peptide length and the presence of the constrained RGD motif in cPRGDA. It was also found that there was no significant difference in the IC_{50} of cPRGDA compared to amide-cPRGDK.

Confocal Microscopy. Confocal microscopy investigated the specific binding of the fluorescein-labeled cPRGDA (**13**) and cPRGDAA (**14**) peptides to the human $\alpha_V\beta_3$ integrin receptor of U87 glioblastoma cells. These studies showed that cPRGDA, cPRGDAA, and the amide-cPRGDK (**23**) each bound to U87 cells (Figure 3A,C,D) but none bound to HT-29 cells (Figure 3G,I,J). The cPRDGA scramble control (**15**) showed nonspecific binding to U87 cells (Figure 3B) but not to HT-29 cells (Figure 3H). The targeting specificity of cPRGDA and cPRGDAA was investigated by blocking the $\alpha_V\beta_3$ integrin receptor of U87 cells with a 50-fold molar excess of the linear RGD peptide (**20**). This blocking reduced specific $\alpha_V\beta_3$ integrin binding for both RGD-containing macrocycles, but the remaining fluorescence signals suggested additional nonspecific binding (Figure 3E,F).

DISCUSSION

The aziridine aldehyde-driven cyclization method has been successfully developed to synthesize functional $\alpha_V\beta_3$ integrin-targeting fluorescein-labeled macrocycles. We were able to show that increasing the peptide length (from five to six residues) and switching the Gly and Asp residues in the middle of the sequence did not affect the aziridine aldehyde-driven cyclization reaction. We used a simple zinc chloride salt to catalyze the sulfhydryl-driven aziridine ring-opening of the exocyclic unsubstituted aziridine handle of our macrocycles by the heterobifunctional linker cysteamine. The versatility of this synthetic strategy was illustrated by conjugating the common radiometal chelator DOTA and the multimodal fluorescent dye/radiometal chelator/photosensitizer pyropheophorbide *a* using NHS-chemistry. This conjugation could be easily adapted to a wide variety of other fluorescent dyes, radiometal chelators, or extended linkers using conventional amide-coupling, the described NHS-chemistry, or by analogous ITC-chemistry.

Aziridine aldehyde-driven macrocyclization reactions showed clear advantages over conventional end-to-end amide cyclization. The former reactions were performed at a much higher

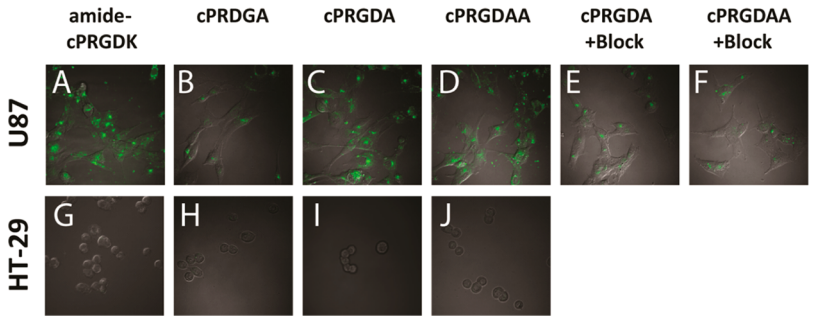

Figure 3. Confocal microscopy fluorescence images merged with DIC showing the differential binding of fluorescein-labeled macrocycles to U87 ($\alpha_V\beta_3$ +) (A–F) and HT-29 ($\alpha_V\beta_3$ −) cells (G–J).

dx.doi.org/10.1021/bc300239a | *Bioconjugate Chem.* 2012, 23, 1387–1395

concentration (50 mM in TFE) wherein no noticeable polymerization was observed. The amide cyclization required high dilution (0.6 mM in DMF) to ensure that amide coupling was predominantly due to intramolecular bonding of the free N- and C-termini within each monomeric linear PRGDK peptide.[30] In addition, the conventional amide cyclization reactions require an additional amino acid to provide a thiol, carboxylic acid, or primary amine for subsequent functional group conjugations. These amino acids should be specially protected and selectively deprotected for functional group conjugation.[7−10] On the contrary; the aziridine aldehyde-driven macrocyclization offers a free amine for conjugation once cysteamine has become bonded to the macrocycle by aziridine ring-opening. We are thereby able to avoid the challenges of protection/deprotection often required after amide cyclization. Finally, after the aziridine ring-opening of the aziridine aldehyde-cyclized macrocycles, the space between the binding motif of the macrocycle and the conjugation site may have allowed the desired receptor binding to proceed without imposing significant steric hindrance.

Analysis of the X-ray crystal structure of integrin-bound cRGDf(N-Me)V shows a significant difference between it and the solution-phase structure proposed by Kessler et al.[26] Cyclic pentapeptides with (LDLDL) relative stereochemistry often adopt a βII′/γ turn architecture in solution. In the case of cRGDf(N-Me)V, Gly occupies the i+1 position of the γ turn while D-Phe occupies the i+1 position of the βII′ turn. The X-ray crystal structure of integrin-bound cRGDf(N-Me)V shows that the γ turn is maintained in the bound state, with a 6.4 Å separation between the Arg and Asp α carbons and a 8.7 Å distance separating the Arg and Asp β carbons. cPRGDA docked to $\alpha_V\beta_3$ and shows that it adopts the same γ turn conformation as the docked cRGDf(N-Me)V, which is critical for the polar side chains of Arg and Asp to engage in receptor binding. The Arg-Asp intercarbon (C^α and C^β) distances of cPRGDA were similar to those of cRGDf(N-Me)V where the Arg-Asp (C^α-C^α) distance is 6.0 Å and the Arg-Asp (C^β-C^β) distance is 8.7 Å. Kessler et al. have shown that the identity of the remaining residues in the peptide are important for structural rigidity, but due to the fact that residues not in the RGD motif do not make contact with the integrin surface, ample room exists to splice different residues and functional handles into the macrocycle sequence,[31] hence the observed binding affinity for cPRGDA.

Computer modeling data showed that cPRGDA contained a similar backbone conformation at the RGD motif to cRGDf(N-Me)V, while cPRGDAA differs significantly. This suggested that the stabilized RGD motif within cPRGDA would contribute to a better binding affinity for the $\alpha_V\beta_3$ integrin receptor compared to cPRGDAA. Competitive cell adhesion assays experimentally showed that the IC_{50} of cPRGDA for $\alpha_V\beta_3$ integrin-overexpressing U87 glioblastoma cells was significantly lower compared to cPRGDAA. This may be explained by the backbone shape and macrocycle ring size differences between the two peptides. It is possible that other RGD-containing pentapeptide sequences cyclized by the aziridine aldehyde-driven reaction may also contain this desired turn at the RGD motif. Nevertheless, confocal analysis showed that both the fluorescein-labeled cPRGDA and cPRGDAA macrocycles could successfully bind to U87 cells for in vitro fluorescence cancer imaging while avoiding binding to HT-29 cells that express low levels of the $\alpha_V\beta_3$ integrin receptor.

The amide-cPRGDK also fulfills the α carbon requirement for a γ-turn-like structure, having a distance of 4.6 Å between the Arg and Asp α carbons. However, the β carbons are much closer than in either PRGDA or cRGDf(N-Me)V where a distance of 7.2 Å separates them. This means that the backbone dihedral angles are significantly different for amide-cPRGDK, which could contribute to a reduction in affinity compared to cRGDf(N-Me)V despite its similar ring size.

Computational docking studies identified the binding mode of cPRGDA and the N^ε-acetyl-lysine analogue of amide-cPRGDK with the extracellular $\alpha_V\beta_3$ integrin receptor. The Lys of amide-cPRGDK was acetylated to mimic the hindrance imposed by fluorescein at the Lys residue in amide-cPRGDK (**23**). We found that both macrocycles interacted with the Asp150 and Asp218 residues of the protein through their respective Arg residues, much the same as cRGDf(N-Me)V. Interestingly, amide-cPRGDK only used two of its three available Arg nitrogen atoms to bind to Asp150 and Asp218, while cPRGDA and cRGDf(N-Me)V used all three nitrogen atoms of their respective Arg residues for optimal integrin binding. In addition, the N^ε-acetyl-lysine residue of amide-cPRGDK interacted with Asp126. Therefore, it was not obvious which binding interaction would have the greatest contribution to the binding affinity of cPRGDA and amide-cPRGDK. Competitive cell adhesion assays experimentally showed that the IC_{50} of cPRGDA for U87 cells was not significantly different compared to amide-cPRGDK. This suggests that the aforementioned difference observed in the described docking studies compensated to create geometries that allowed similar in vitro binding to the $\alpha_V\beta_3$ integrin receptor on U87 cells.

The chemical structures of the cPRGDA, cPRGDAA, and cPRDGA macrocycles are inherently different from analogous peptide macrocycles generated through backbone amide coupling. The aziridine aldehyde-driven cyclization and the subsequent aziridine ring-opening reaction result in the formation of an sp^3-hybridized carbon atom at the non-amino acid portion of the macrocycles. The described geometric and binding affinity comparisons between cPRGDA and amide-cPRGDK are similar to the investigations published by Geyer et al. in 1994.[32] They developed the cyclic peptide cRGDfψ-[CH_2−NH]V that contained a reduced amide bond that imposed geometric differences when compared to the parent cRGDfV, whereas with cRGDfψ[CH_2−NH]V, they found that a β-turn forms between the Val and Asp residues (a γ turn lies between Arg and Asp in potent RGD cyclic peptides). They also found that the structural perturbation caused by the introduction of a reduced amide bond into a cyclic RGD peptide caused a significant drop in activity. This suggests that RGD macrocycles containing only amide bonds would stabilize geometries that result in superior $\alpha_V\beta_3$ integrin binding affinities compared to analogues that do not contain a fully amide-bonded backbone. Interestingly, the binding affinity of cPRGDA to the $\alpha_V\beta_3$ integrin receptor was not significantly different compared to amide-cPRGDK. Though the amino acid residues of cPRGDA and amide-cPRGDK were not identical, it could be inferred that the sp^3 carbon-containing macrocycles generated through aziridine aldehyde-driven cyclization and subsequent aziridine ring-opening may not hinder the binding affinity of cyclic RGD sequences to the same extent as the aforementioned study when compared to analogues that contain only amide bonds.

We have shown that the aziridine aldehyde-driven cyclization modulated the geometry of similar five- and six-membered

RGD macrocycles and was responsible for tuning the binding affinity of cPRGDA and cPRGDAA for the $\alpha_V\beta_3$ integrin receptor on U87 cancer cells. It is possible that the geometry-modulating ability of this macrocyclization reaction can create other RGD-based macrocycles that have varying binding affinities and also varying specificities to different integrin subtypes that are also overexpressed by cancers. This geometry-modulating ability could also be extended to other cancer biomarker-targeting peptide sequences. Using our current modification strategy, these new potential macrocycles could then be conjugated to a variety of functionalities for additional imaging and therapeutic applications.

CONCLUSION

We have created a versatile strategy for conjugating a common fluorescent dye to RGD-containing $\alpha_V\beta_3$ integrin receptor-targeting macrocycles which were cyclized by the aziridine aldehyde-driven reaction. This same general method was used to conjugate the commonly used radiometal chelator DOTA and the multifunctional porphyrin pyropheophorbide to a novel RGD-containing macrocycle to display the versatility of our conjugation strategy. Computer modeling studies showed that the aziridine aldehyde-driven cyclization modulated the geometry of similar five and six amino acid-containing RGD macrocycles. This cyclization chemistry was responsible for stabilizing a γ turn at the RGD motif of cPRGDA. Though each fluorescein-labeled RGD-containing peptide specifically targeted the $\alpha_V\beta_3$ integrin receptor of U87 glioblastoma cells in vitro, it is likely that a stabilized γ turn and the significantly shorter Pro-C^{α}-Asp-C^{α} distance were responsible for improving the binding affinity of cPRGDA compared to cPRGDAA. Future studies should continue using pentapeptides to constrain the RGD motif into an active conformation and replace the C-terminal Ala with other natural or synthetic L- or D-amino acid residues to further improve $\alpha_V\beta_3$ integrin binding or possibly to selectively target different integrin subtypes. Additional studies could use the aziridine aldehyde-driven cyclization chemistry to modulate the geometry of other cancer biomarker-targeting sequences and utilize the described modification strategy for a variety of cancer imaging and therapeutic applications.

ASSOCIATED CONTENT

Supporting Information

HPLC-MS characterization spectra for all the modified macrocycles. This material is available free of charge via the Internet at http://pubs.acs.org.

AUTHOR INFORMATION

Corresponding Author

*Prof. Andrei K. Yudin: Tel. 416-946-5042; E-mail: ayudin@chem.utoronto.ca. Prof. Gang Zheng: Tel. 416-581-7666, Fax 416-581-7667, E-mail: gang.zheng@uhnres.utoronto.ca.

Notes

The authors declare no competing financial interest.

ACKNOWLEDGMENTS

G.Z. and A.Y. thanks NSERC and CIHR for financial support of this project. Support from Princess Margaret Hospital Foundation is also acknowledged.

REFERENCES

(1) Hili, R., Rai, V., and Yudin, A. K. (2010) Macrocyclization of linear peptides enabled by amphoteric molecules. *J. Am. Chem. Soc. 132*, 2889−2891.
(2) Rotstein, B. H., Mourtada, R., Kelley, S. O., and Yudin, A. K. (2011) Solvatochromic reagents for multicomponent reactions and their utility in the development of cell-permeable macrocyclic peptide vectors. *Chem.—Eur. J. 17* (44), 12257−12261.
(3) Rotstein, B. H., Winternheimer, D. J., Yin, L. M., Deber, C. M., and Yudin, A. K. (2012) Thioester-isocyanides: versatile reagents for the synthesis of cycle-tail peptides. *Chem. Commun. 48* (31), 3775−3777.
(4) Zhang, Q.-J., Lindquist, Y., Levitsky, V., and Masucci, M. G. (1996) Solvent exposed side chains of peptides bound to HLA A*1101 have similar effects on the reactivity of alloantibodies and specific TCR. *Int. Immunol. 8* (6), 927−938.
(5) Zhang, X., Xiong, Z., Wu, Y., Cai, W., Tseng, J. R., Gambhir, S. S., and Chen, X. (2006) Quantitative PET imaging of tumor integrin $\alpha_V\beta_3$ expression with ^{18}F-FRGD2. *J. Nucl. Med. 47*, 113−121.
(6) Ratcliffe, K. E., Fraser, H. M., Sellar, R., Rivier, J., and Millar, R. P. (2006) Bifunctional gonadotropin-releasing hormone antagonist-progesterone analogs with increased efficacy and duration of action. *Endocrinology 147* (1), 571−579.
(7) Isidro-Llobet, A., Álvarez, M., and Albericio, F. (2009) Amino acid-protecting groups. *Chem. Rev. 109*, 2455−2504.
(8) Kopple, K. D. (1972) Synthesis of cyclic peptides. *J. Pharm. Sci. 61* (9), 1345−1356.
(9) Harris, K. M., Flemer, S., Jr., and Hondal, R. J. (2007) Studies on deprotection of cysteine and selenocysteine side-chain protecting groups. *J. Pept. Sci. 13*, 81−93.
(10) Guzmán, F., Barberis, S., and Illanes, A. (2007) Peptide synthesis: Chemical or enzymatic. *Electron. J. Biotechnol. 10* (2), 279−314.
(11) Ye, T., and Chen, X. (2011) Integrin targeting for tumor optical imaging. *Theranostics 1*, 102−126.
(12) Ruoslahti, E. (1996) RGD and other recognition sequences for integrins. *Annu. Rev. Cell Dev. Biol. 12*, 697−715.
(13) Montet, X., Montet-Abou, K., Reynolds, F., Weissleder, R., and Josephson, L. (2006) Nanoparticle imaging of integrins on tumor cells. *Neoplasia 8* (3), 214−222.
(14) Liu, Z., Wang, F., and Chen, X. (2008) Integrin $\alpha_V\beta_3$-targeted cancer therapy. *Drug Dev. Res. 69*, 329−339.
(15) Zhou, Y., Chakraborty, S., and Liu, S. (2011) Radiolabeled cyclic RGD peptides as radiotracers for imaging tumors and thrombosis by SPECT. *Theranostics 1*, 58−82.
(16) Dechantsreiter, M. A., Planker, E., Mathä, B., Lohof, E., Hölzemann, G., Jonczyk, A., Goodman, S. L., and Kessler, H. (1999) *N*-Methylated cyclic RGD peptides as highly active and selective $\alpha_V\beta_3$ integrin antagonists. *J. Med. Chem. 42*, 3033−3040.
(17) Gilbert, M. R., Kuhn, J., Lamborn, K. R., Lieberman, F., Wen, P. Y., Mehta, M., Cloughesy, T., Lassman, A. B., DeAngelis, L. M., Chang, S., and Prados, M. (2012) Cilengitide in patients with recurrent glioblastoma: the results of NABTC 03−02, a phase II trial with measures of treatment delivery. *J. Neuro-Oncol. 106* (1), 147−153.
(18) Hariharan, S., Gustafson, D., Holden, S., McConkey, D., Davis, D., Morrow, M., Basche, M., Gore, L., Zang, C., O'Bryant, C. L., Baron, A., Gallemann, D., Colevas, D., and Eckhardt, S. G. (2007) Assessment of the biological and pharmacological effects of the $\alpha_V\beta_3$ and $\alpha_V\beta_5$ integrin receptor antagonist, cilengitide (EMD 121974), in patients with advanced solid tumors. *Ann. Oncol. 18*, 1400−1407.
(19) Zhang, M., Zhang, Z., Blessington, D., Li, H., Busch, T. M., Madrak, V., Miles, J., Chance, B., Glickson, J. D., and Zheng, G. (2003) Pyropheophorbide 2-deoxyglucosamide: A new photosensitizer targeting glucose transporters. *Bioconjugate Chem. 14*, 709−714.
(20) Rotstein, B. H., Rai, V., Hili, R., and Yudin, A. K. (2010) Synthesis of peptide macrocycles using unprotected amino aldehydes. *Nat. Prot. 5* (11), 1813−1822.
(21) Mohamadi, F., Richard, N. G. J., Guida, W. C., Liskamp, R., Lipton, M., Caufield, C., Chang, G., Hendrickson, T., and Still, W. C.

(1990) MacroModel - an Integrated software system for modeling organic and bioorganic molecules using molecular mechanics. *J. Comput. Chem. 11* (4), 440−467.
(22) Jorgensen, W. L., and Tirado-Rives, J. (2005) Potential energy functions for atomic-level simulations of water and organic and biomolecular systems. *Proc. Natl. Acad. Sci. U.S.A. 102* (19), 6665−6670.
(23) Tsui, V., and D., A. (2001) Case, theory and applications of the generalized Born solvation model in macromolecular simulations. *Biopolymers 56* (4), 275−291.
(24) Hastings, W. K. (1970) Monte-Carlo sampling methods using Markov chains and their applications. *Biometrika 57*, 97−109.
(25) Metropolis, N., Rosenbluth, A. W., Rosenbluth, M. N., Teller, A. H., and Teller, E. (1953) Equations of state calculations by fast computing machines. *J. Chem. Phys. 21* (6), 1087−1092.
(26) Xiong, J. P., Stehle, T., Zhang, R., Joachimiak, A., Frech, M., Goodman, S. L., and Arnaout, M. A. (2002) Crystal structure of the extracellular segment of integrin $\alpha_v\beta_3$ in complex with an Arg-Gly-Asp ligand. *Science 296*, 151−155.
(27) Wang, W., Wu, Q., Pasuelo, M., McMurray, J. S., and Li, C. (2005) Probing for integrin $\alpha_v\beta_3$ binding of RGD peptides using fluorescence polarization. *Bioconjugate Chem. 16*, 729−734.
(28) Liu, Z., Jia, B., Shi, J., Jin, X., Zhao, H., Li, F., Liu, S., and Wang, F. (2010) Tumor uptake of the RGD dimeric probe 99mTc-G3−2P4-RGD2 is correlated with integrin $\alpha_v\beta_3$ expressed on both tumor cells and neovasculature. *Bioconjugate Chem. 21*, 548−555.
(29) Rüegg, C., Hasmim, M., Lejeune, F. J., and Alghisi, G. C. (2006) Antiangiogenic peptides and proteins: From experimental tools to clinical drugs. *Biochim. Biophys. Acta 1765*, 155−177.
(30) Davies, J. S. (2003) The cyclization of peptides and depsipeptides. *J. Pept. Sci. 9*, 471−501.
(31) Pfaff, M., Tanglemann, K., Müller, B., Gurrath, M., Müller, G., Kessler, H., Timpl, R., and Engel, J. (1994) Selective recognition of cyclic RGD peptides of NMR defined conformation by $\alpha_{IIb}\beta_3$, $\alpha_v\beta_3$, and $\alpha_5\beta_1$ integrins. *J. Biol. Chem. 269* (32), 20232−20238.
(32) Geyer, A., Müller, G., and Kessler, H. (1994) Conformational analysis of a cyclic RGD peptide containing a ψ[CH2-NH] bond: A positional shift in backbone structure caused by a single dipeptide mimetic. *J. Am. Chem. Soc. 116*, 7735−7743.